

INFLUENCE OF INTERNAL WAVES ON SOUND PROPAGATION
IN THE SOFAR CHANNEL

by

H.H. Essen
University of Hamburg
Germany

ABSTRACT

In this paper theoretical investigations due to the influence of internal waves to sound propagation in the SOFAR-channel are presented. The undisturbed acoustic field is described by a normal-mode model. The disturbance by internal waves is considered in the two limits.

1) The internal wavelengths are large compared with acoustic wavelengths. The result is a phase fluctuation for each individual mode. Interference of the total mode field yields amplitude fluctuations as well.

2) Internal wavelengths cannot be considered large compared with acoustic wavelengths. Then acoustic energy is transferred from mode to mode. This problem is treated by the theory of resonant wave-wave interaction (Bragg scattering).

Numerical results are presented and compared with published experiments.

In recent years considerable experimental efforts have been made in determining the spectral distribution of internal waves in the deep ocean. For this usually direct measurements with current meters and temperature sensors are applied. Acoustic CW measurements carried out over a fixed range show phase and amplitude fluctuations with internal-wave frequencies. Thus due to internal waves these acoustic measurements can be understood as a method of remote sensing.

The periods of the motions within the ocean are large compared with acoustic periods and therefore the acoustic pressure p of a fixed-range receiving hydrophone can be described by,

$$p(t) = A(t) \cdot \cos\{2\pi \nu t - \phi(t)\}$$

where ν is the frequency of the CW source, and the amplitude $A(t)$ and phase $\phi(t)$ are slowly varying, e.g. caused by internal waves.

In 1974 results from two different fixed-range measurements in the deep ocean between the Bahamas and Bermudas were published by STANFORD (1974) and CLARK and KRONENGOLD (1974). Stanford's measurements were carried out in 1968, and the frequency of the source was 367 cps. Fig. 1 shows power spectra of the acoustic amplitude $A(t)$ and phase $\phi(t)$. In 1971 Clark and Kronengold used the same experimental site, the source frequency was 406 cps. The main progress was the sample length of 20 days as opposed to Stanford's three-day samples. Thus Clark and Kronengold's data allow the resolution of tidal periods. Fig. 2 shows the amplitude spectra of the acoustic amplitude $A(t)$ and phase $\phi(t)$ from two different hydrophones.

In this paper theoretical investigations are presented in order to interpret the experimental results.

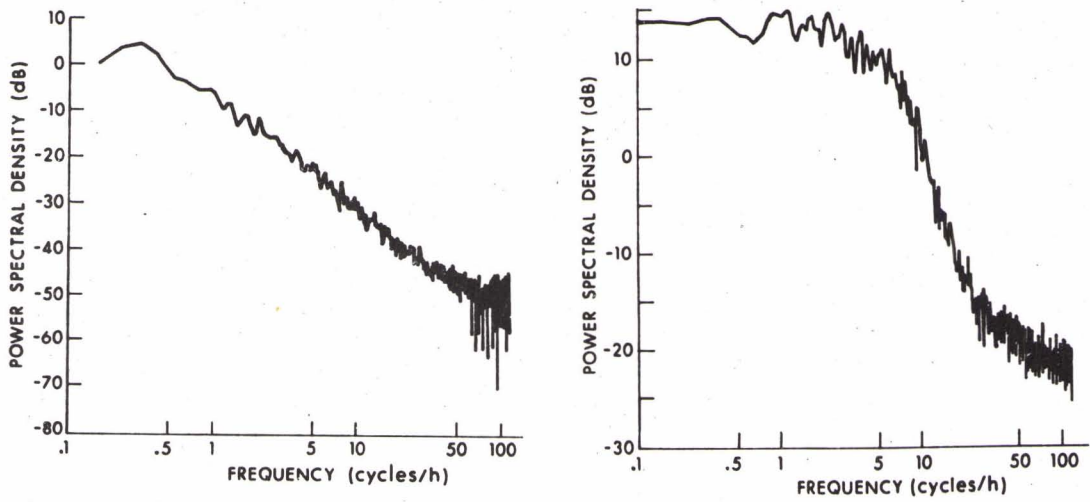


FIG. 1 POWER SPECTRA OF ACOUSTIC PHASE $\Phi(t)$ (left) AND ACOUSTIC AMPLITUDE $A(t)$ (right), FROM STANFORD (1974)

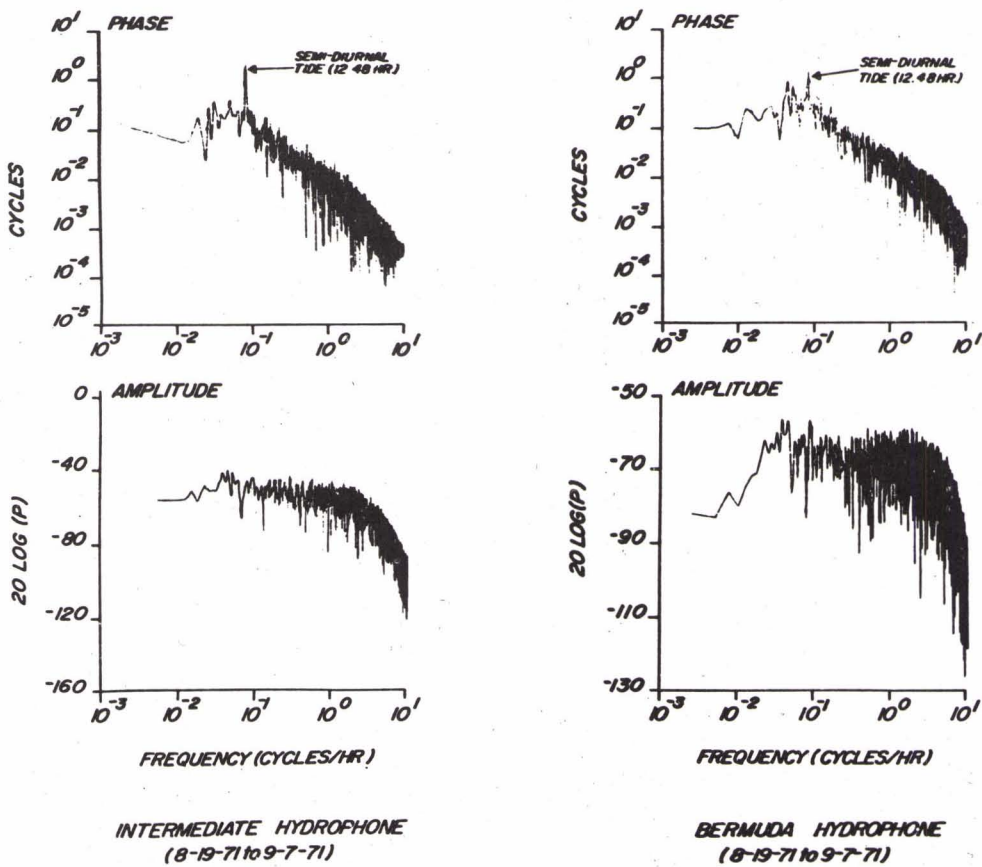


FIG. 2 AMPLITUDE SPECTRA OF ACOUSTIC PHASE $\Phi(t)$ AND ACOUSTIC AMPLITUDE $A(t)$, FROM CLARK AND KRONENGOLD (1974)

The undisturbed sound propagation is described by a normal-mode model. In Fig. 3 sound-velocity profiles measured along the acoustic range and a theoretical model $c_0(x_3)$ are shown. The theoretical model is,

$$c_0(x_3) = 1.49 \text{ km/s} \begin{cases} \cdot [1 - 0.21 \cdot (x_3 + 0.25h)/h]^{-\frac{1}{2}} & , x_3 \geq -0.25h \\ \cdot [1 + 0.13 \cdot (x_3 + 0.25h)/h]^{-\frac{1}{2}} & , x_3 \leq -0.25h \end{cases}$$

$h = 5 \text{ km}$ water depth

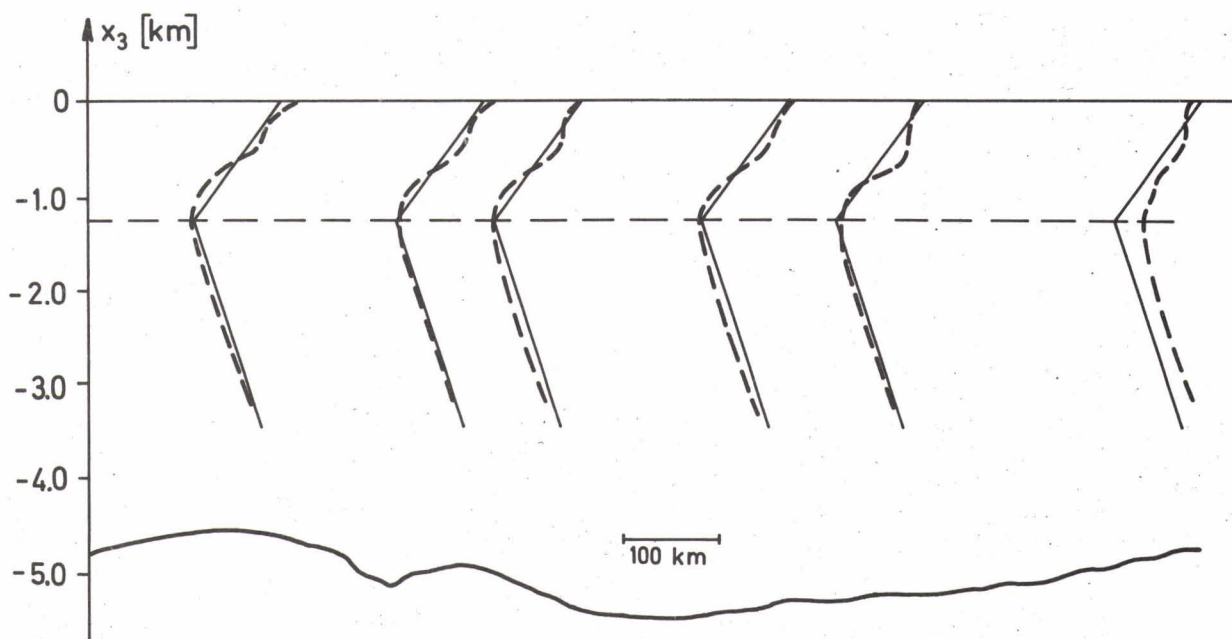


FIG. 3 SOUND VELOCITY AS FUNCTION OF DEPTH

--- measured by CLARK and KRONENGOLD (1974)
 — theoretical model

From this model the acoustic normal-mode solutions $\psi_n(x_3)$ are given by Airy functions. The first 8 modes are plotted in Fig. 4.

The disturbance of the acoustic normal-mode field is considered in the two limits:

The internal wavelengths are large compared with acoustic wavelengths. The phase fluctuations of the single modes due to travel-time fluctuations may be computed. Interactions between the modes are negligible.

Internal wavelengths can not be considered large compared with

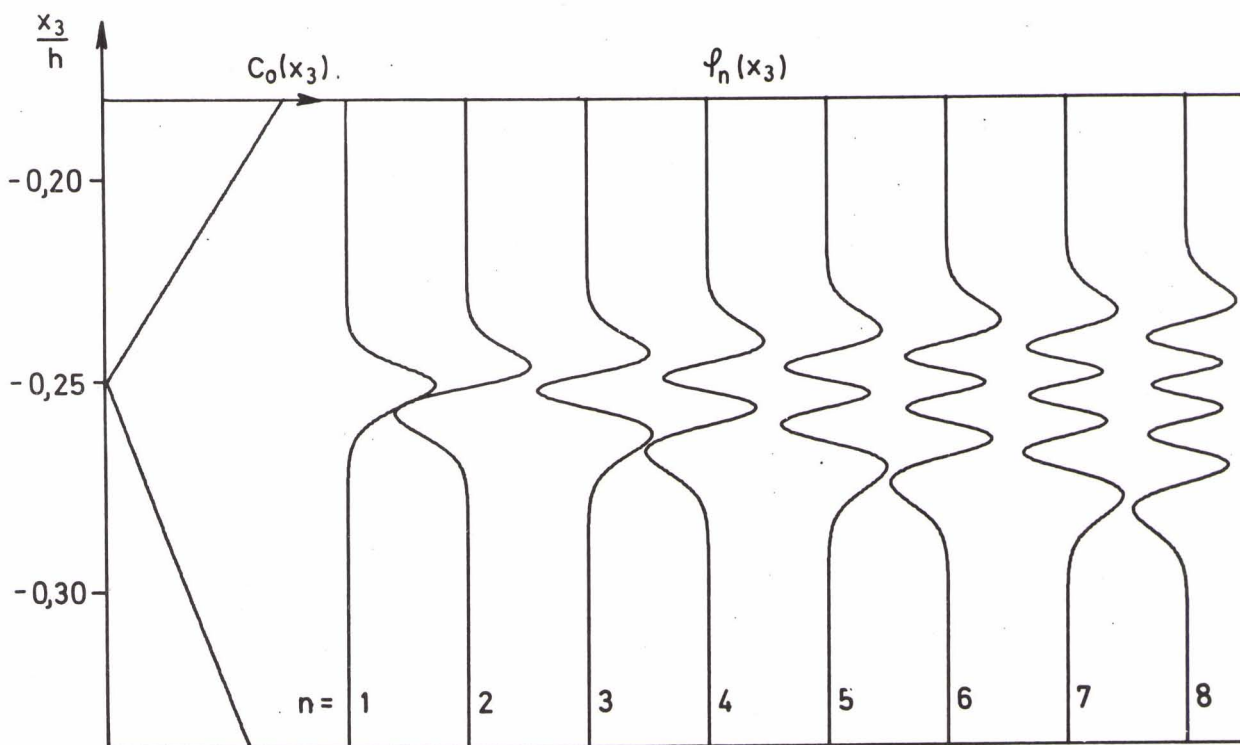


FIG. 4 COMPUTED NORMAL-MODE FUNCTIONS $\varphi_n(x_3)$ FOR AN ACOUSTIC FREQUENCY OF 400 cps

acoustic wavelengths. This problem is treated by the theory of wave-wave interaction (Bragg scattering), which yields an energy transfer from mode to mode.

Long internal waves

With regard to trapped SOFAR propagation boundary effects are negligible. In the limit of oceanic disturbances large compared with acoustic wavelengths the disturbed wave equation may be written,

$$\frac{1}{(c_0 + c_s)^2} \left(\frac{\partial}{\partial t} + \mu_{s_i} \frac{\partial}{\partial x_i} \right)^2 p - \frac{\partial^2 p}{\partial x_i \partial x_i} = 0 \quad (i = 1, 2, 3)$$

μ_{s_i} particle velocity of oceanic motions

c_s sound-velocity disturbances by oceanic motions

The disturbed propagation problem is treated by a normal-mode ansatz, where the mode amplitudes as well as the vertical mode functions are slowly range dependent. A WKB approximation is made for the amplitudes, and the vertical eigenvalue problem is

solved by a perturbation expansion. In lowest order these approximations yield the phase fluctuations of the single modes. These phase fluctuations are obviously caused by travel-time fluctuations due to oceanic motions.

The received signal is a superposition of many modes. Generally the phase changes differ from mode to mode and the relation between the mode-phase changes and the amplitude and phase changes of the received signal becomes nonlinear. In this case it is impossible to get an explicit relationship between the power spectrum of the oceanic motions and the power spectra of the received acoustic amplitude and phase. This difficulty is overcome by the assumption that only a finite number of modes contribute to the received signal. Considering an oceanic internal-wave field numerical computations yield small phase differences of adjacent modes. Expanding in terms of these small phase differences the received amplitude becomes constant in lowest order and the received phase is equal to the mean normal-mode phase.

Theoretical power spectra of the normal-mode phase are shown in Fig. 5. The oceanic motions are described by a random internal-wave field in an ocean with constant Brunt-Väisälä frequency. In agreement with GARRETT and MUNK (1972) the spectral density is assumed proportional to ω^{-2} and isotropic in the horizontal coordinates. Considering barotropic motions only, the spectra become independent of the acoustic mode number. That is, the phase changes of all acoustic modes are nearly the same. From this fact the lack of the tidal peak in the observed spectrum of the acoustic amplitude may be understood, see Fig. 2. Considering the barotropic and the first baroclinic modes as well, the theoretical spectra become dependent on the acoustic mode number n .

The slope of the theoretical spectra in Fig. 5 is $\omega^{-1.3}$, in good agreement with the measurements.

Short internal waves

In the case of acoustic propagation through a short-scale oceanic wave field the acoustic wave equation becomes more complicated. Considering a superposition of oceanic and acoustic field and

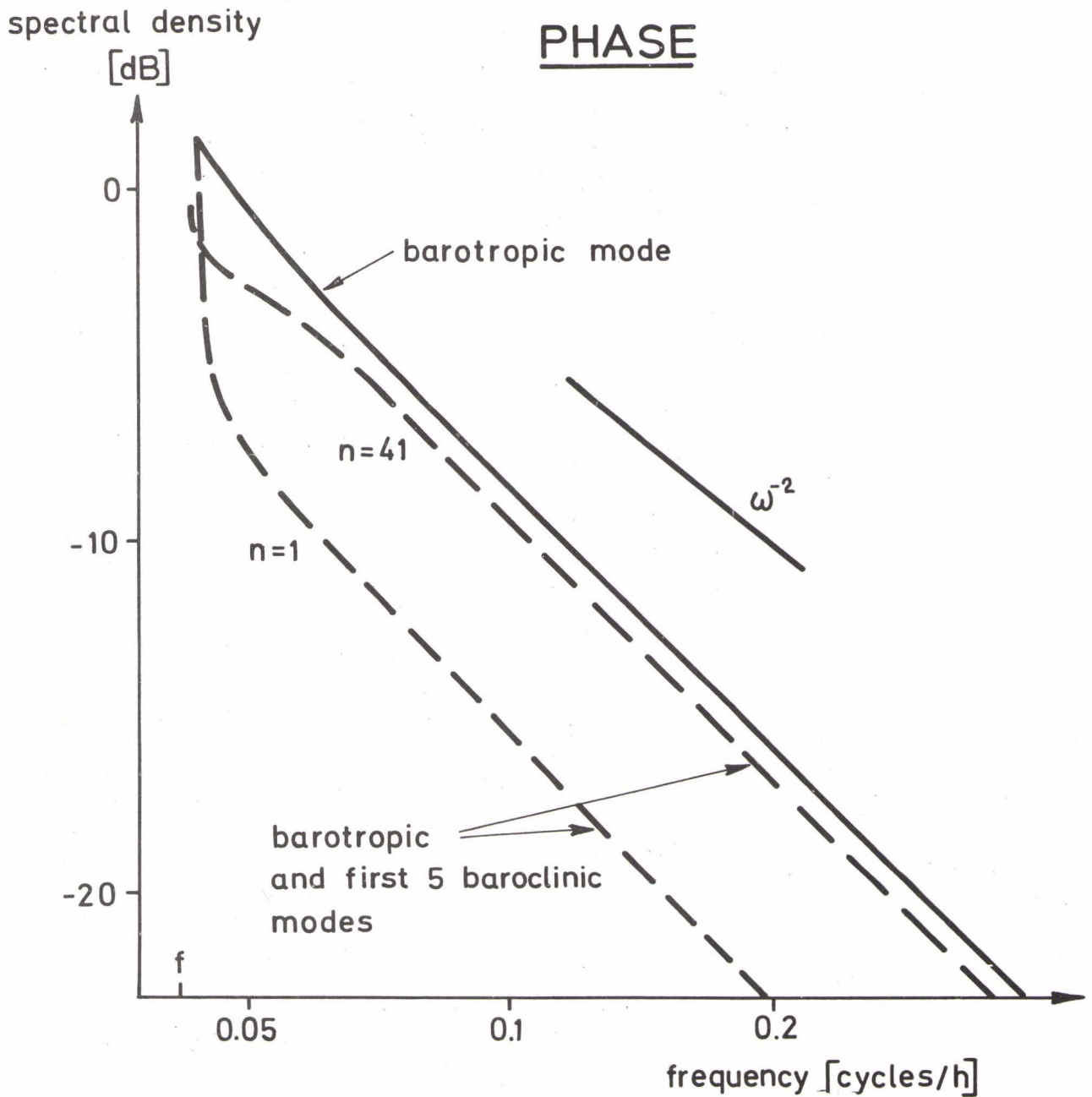


FIG. 5 COMPUTED POWER SPECTRA OF THE ACOUSTIC PHASE $\Phi(t)$ FOR A SOURCE FREQUENCY OF 400 cps

inserting into the hydrodynamic equations, one obtains,

$$\frac{1}{c_0^2} \frac{\partial^2 p}{\partial t^2} - \frac{\partial^2 p}{\partial x_i \partial x_i} - 2 \frac{c_s}{c_0^3} \frac{\partial^2 p}{\partial t^2} - 2 g_0 \frac{\partial}{\partial x_j} \left(\mu_{sj} \frac{\partial \mu_j}{\partial x_i} \right) + \frac{1}{g_0} \frac{\partial \rho_s}{\partial x_i} \frac{\partial p}{\partial x_i} + \dots = 0$$

- u_i acoustic particle velocity
- ρ_0 mean density
- ρ_i density fluctuations due to oceanic motions

where some small terms have been neglected and only quadratic coupling of acoustic to oceanic field is taken into account.

Solutions of the propagation problem are found by a perturbation expansion of the acoustic pressure,

$$p = p^{(0)} + p^{(1)} + \dots$$

The zero order describes the undisturbed normal-mode field. The first-order equations are determined by the quadratic coupling of the zero-order acoustic field to the oceanic field. From this the solutions yield scattered acoustic waves with the sum and difference of the interacting horizontal wavenumbers (α) and frequencies (ω),

$$\alpha_n' = \alpha_n \pm \alpha_s \quad (\alpha = 1, 2)$$

$$\omega' = \omega \pm \omega_s$$

The solutions become resonant if the scattered wavenumber α_n' and frequency ω' fulfill the normal-mode relation. And from this resonant solutions the energy transfer from mode to mode can be computed.

For a source radiating into a certain horizontal angular range it is now the problem to add all scattered and frequency-shifted modes reaching the receiving hydrophone from the different horizontal directions. This was done in order to compute the power spectra of the acoustic amplitude, shown in Fig. 6. The oceanic motions are described by a random internal-wave field. The Brunt-Väisälä frequency was assumed constant (\bar{N}) within the upper and zero within the lower part of the ocean. For the spectral distribution the Garrett-Munk model was considered.

References:

Stanford, G.E.: Low-frequency fluctuations of a CW signal in the ocean, J. Acoust. Soc. Am. 55, 968-977, 1974

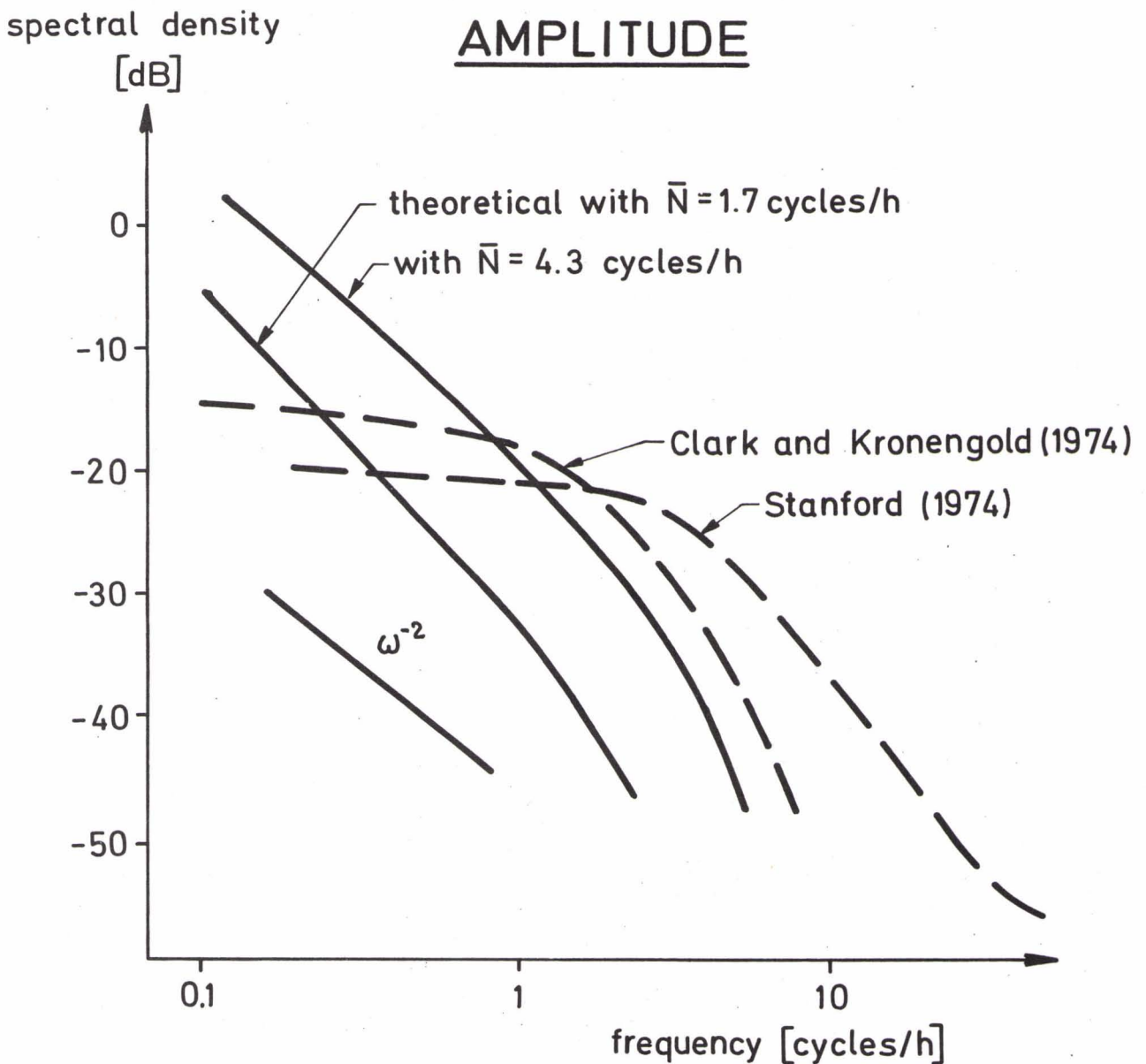


FIG. 6 COMPARISON OF MEASURED AND COMPUTED POWER SPECTRA OF THE ACOUSTIC AMPLITUDE $A(t)$ FOR A SOURCE FREQUENCY OF 400 cps

Clark, J.G., and Kronengold, M.: Long-period fluctuations of CW signals in deep and shallow water, *J. Acoust. Soc. Am.* 56, 1071-1083, 1974

Garrett, Ch., and Munk, W.: Space-Time Scales of Internal Waves, *Geophys. Fluid Dyn.* 3, 225-264, 1972